Study of relationship between ENSO/IODM and NDVI in Western Pacific regions

○**Bannu, Josaphat Tetuko Sri Sumantyo, Hiroaki Kuze**
Center for Environmental Remote Sensing (CEReS), Chiba University,
1-33 Yayoi-cho, Inage-ku, Chiba 263-8522, Japan
E-mail : bannu@graduate.chiba-u.jp

Abstract: We examine the correlation between the Niño-3,4/IODM indices that describe the SST anomalies on a global scale and the regional NDVI index in the Western Pacific including Indonesia. An approach is adopted that enhances NDVI anomalies relative to the long-term climatology on the global and regional scales. We find a negative NDVI anomaly for most of the region during the El Niño/IODM events, whereas for the non-El Nino/IODM events, positive NDVI anomalies are observed over most regions. Also we identify the possible factors that may play a role in the different NDVI responses to the different El Niño/IODM case. Especially the response of vegetation may depend upon the climate conditions prior to the El Niño/IODM events. In this context, droughts are particularly well suited to early warning systems because the disasters have a slow onset.

Keywords: El Niño, IODM, Rainfall, NDVI, cloud pattern

1. Introduction

Modeling studies (Miller et al., 1992) and observations (McBride et al., 2003) have indicated that small changes in the SST within the Indonesian Maritime Continent can result in significant changes in rainfall patterns across the Indo-Pacific region. On the planetary scale, it is expected that Indonesian rainfall is strongly affected by both the El Niño-Southern Oscillation (ENSO) and the Indian Ocean Dipole (IODM) phenomena. The ENSO and IODM events, in turn, are strongly influenced by radiative and cloud processes in the Tropical Western Pacific (TWP). It is expected that variability of cloud pattern may lead to variability of other climate indicators such as precipitation, evaporation and ocean stream flow.

Satellite information has contributed to improving our understanding of the spatial variability of hydro-climatology. Vegetation activity is tightly coupled with climate and it controls water budget in basins on a wide range of space–time scales. The purpose of the present paper is to elucidate the temporal and spatial relations between El Niño/IODM indices with the cloud pattern, precipitation, and vegetation conditions in Indonesia and related areas.

2. Data and Methodology

The normalized difference vegetation index (NDVI) is defined as NDVI = $(\rho_2-\rho_1)$ / $(\rho_2+\rho_1)$, where, ρ_1 and ρ_2 are the reflectance in the visible (VIS) and the near infrared (IR) band, respectively. The dataset provided by the Global Inventory Monitoring and Modeling Systems (GIMMS) group is based on a 23-year (1981–2003) satellite record of bi-monthly changes in terrestrial vegetation. Its new features include reduced NDVI variations arising from calibration, view geometry, volcanic aerosols, and other effects not related to actual vegetation change (Anyamba et al., 2001). The original GIMMS dataset consists of compositions during 15 days. In order to extract more genuine NDVI variations, first, twice monthly images were averaged to produce one image per month. Second, monthly climatology images were constructed by averaging the monthly data for 23 years. Third, NDVI anomaly or NDVI deviations from the climatology images are calculated for all months from 1981 to 2003. Negative NDVI deviation values indicate lower than average greenness, while positive deviations indicate more green conditions

The Geostationary Meteorological Satellites (GMS-5) captured the hourly cloud pattern over the TWP. We analyze hourly 1-km visible image (0.55-0.90 μm), 5-km infrared-1 (IR1; 10.5-11.5 μm), infrared-2 (IR2; 11.5-12.5 μm) and infrared-3 (Water Vapor; 6.5-7.0 μm) radiance images using the Atmospheric Window Method (AWM), a method proposed by Meteorological Satellite Center of Japan Meteorological Agency (MSC, 2002).

3. Results and Discussion

3.1 Sea Surface Temperature (SST) pattern

The occurrence of El Niño and/or La Niña conditions is represented by the SST anomalies Here we retrieve the SST from the ERSST v2 dataset (Smith & Reynolds, 2005). Figure 1 shows the monthly-average SST during the El Niño/La Niña event of September 1997/September 1998. The El Niño case (Fig. 1a) shows cold areas around the Indonesian region, though relatively warm SSTs are found in the Central Pacific and Indian Oceans.

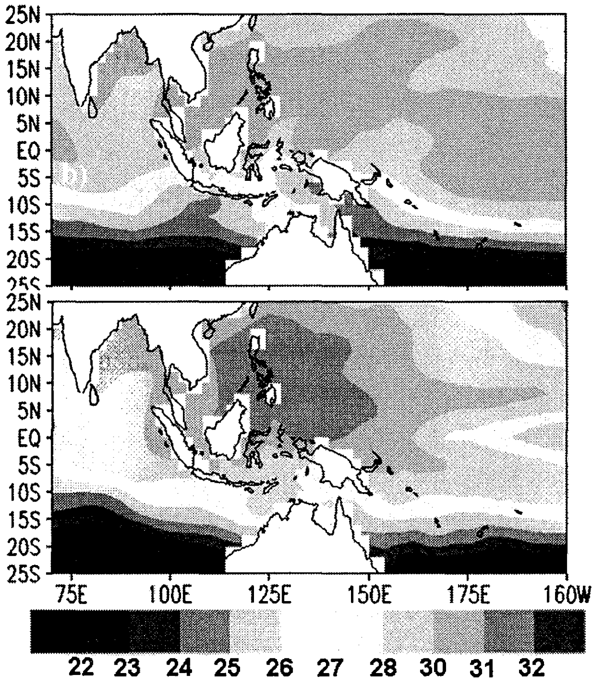

Figure 1 Monthly SST (°C) obtained from ERSST v2 reanalysis dataset (Smith & Reynolds, 2005) surrounding Indonesian region during: a) the El Niño event (September 1, 1997), and b) the La Niña event (September 1, 1998).

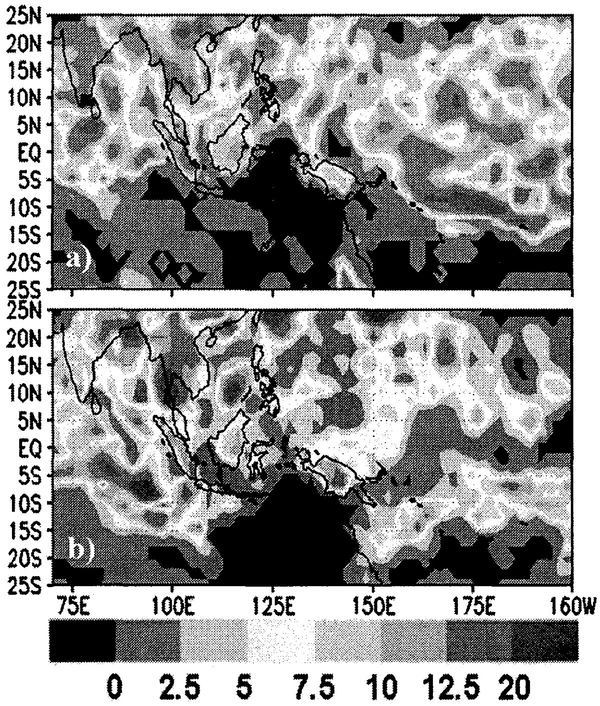

Figure 2 Daily rainfall (mm/day) obtained from NCEP/NCAR reanalysis dataset (Kalnay et al, 1996) during: a) the El Niño event (September 1, 1997), and b) the La Niña event (September 1, 1998).

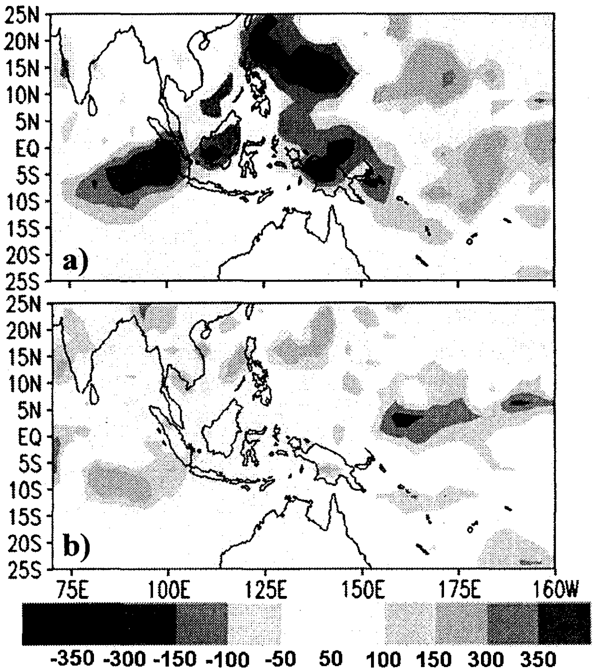

Figure 3 Monthly rainfall anomaly (mm/month) obtained from GCPC v2 dataset (Adler et al, 2003) during: a) the El Niño event (September 1997), and b) the La Niña event (September 1998).

The opposite condition appears in the La Niña condition (Fig. 1b).

The corresponding daily rainfall (non-anomaly) and the monthly rainfall anomalies in the region are depicted in Figs. 2 and 3, respectively. Warm SSTs around the islands of the Maritime Continent lead to vast amounts of evaporation and deep convective cells over the region. The anomaly plot in Fig. 3 well characterizes the influence of El Niño/La Niña conditions on the convective activity.

3.2 Cloud pattern

Figure 4 illustrates the cloud distributions over tropics for the 1997 El Niño (a) and 1998 La Niña (b) conditions derived from the differential IR images of GMS-5. At 00UTC on September 1, 2007 (Fig. 4a), a high cloud fraction is seen over equatorial central Pacific area with a low coverage over the Indonesian region, associated with the dry conditions there. The apparent cloud increase over Kalimantan and Sumatra is presumably due to smoke clouds caused by forest fire events.

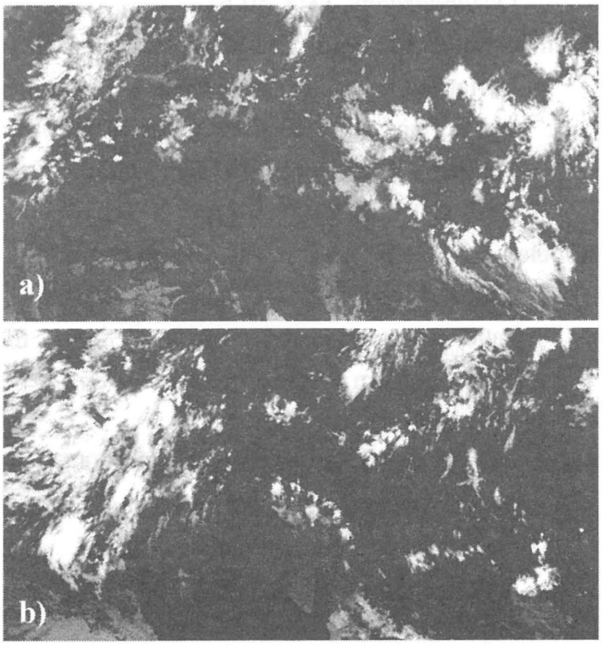

Figure 4 Hourly convective cloud patterns using Infrared differential image taken by GMS-5 at 00UTC on: a) September 1, 1997 (El Niño) and b) September 1, 1998 (La Niña).

The patterns in Fig. 4 also indicate that over the Indonesian region, there is less convection and fewer cold clouds during the El Niño (September 1997) as compared to the La Niña (September 1998) conditions. Nevertheless, in the Western Pacific, there is a greater spatial extent of cold temperatures during the El Niño of 1997 compared to the La Niña conditions of 1998. It is possible that these differences are due to the very cold cloud tops associated with the very intense deep convection prevalent over the ocean in comparison to the weaker, less intense deep convection over the land. Further studies on the diurnal cycle will be useful for the understanding of this cloud behavior.

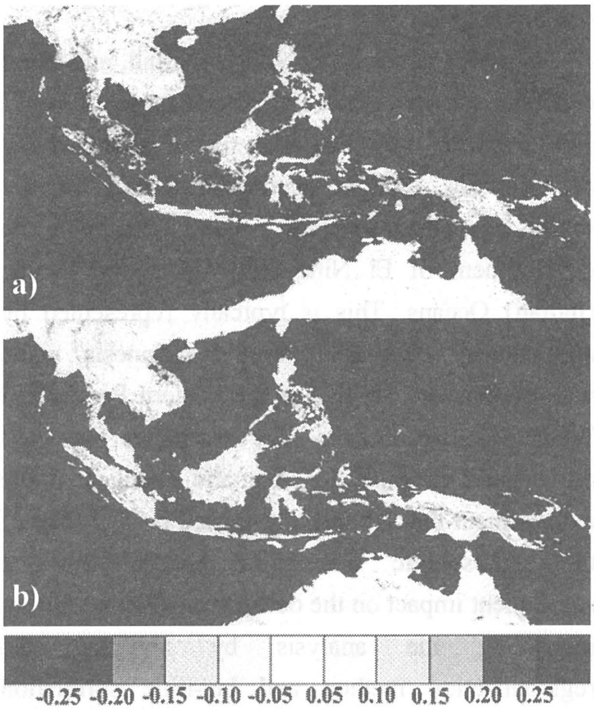

Figure 5 Monthly AVHRR-NDVI anomaly images of Indonesia region during: a) the El Niño event (September 1997) and the La Niña event (September 1998).

3.3 NDVI anomaly

Monthly NDVI anomalies for the El Niño (September 1997) and La Niña (September 1998) events are shown in Fig. 5. Changes in rainfall patterns induced by the El Niño and IODM conditions exert significant effects on biomass production of Indonesia area. This effect can be revealed by NDVI anomaly patterns, particularly in equatorial western part of Indonesia (Kalimantan and Sumatera) where the ENSO–rainfall linkage is most pronounced. A reversal was found in the NDVI response from negative during the El Niño event in 1997/98 to positive during the La Niña event in 1998/99. This reversal can partly be attributed to the east–west reversal in SST gradients in the Pacific Ocean, but more significantly to the changes in the SST anomaly patterns in the equatorial western Indian Ocean. The results of the lag-correlation analysis between the NDVI anomalies and the ENSO/IODM indices will be given in the presentation.

4. Conclusion

Changes in the SST, NDVI, rainfall, and cloud coverage clearly indicate the occurrence of an El Niño event in 1997. Our analysis has indicated that in Indonesia, drought conditions during the dry season typically take place in conjunction with the development of El Niño (IODM) in the Pacific (Indian) Oceans. This is typically represented by anomalously cold SST around Indonesia while warm anomalies develop in the Eastern Pacific and Western Indian Oceans. The anomalies presented are a good example for dramatic changes of the environment that are initially caused by a change of the atmospheric circulation pattern and its subsequent impact on the ocean state. We are further improving the analysis by applying the regionalization method and lag-time correlation analysis (Bannu et al, 2007) among the relevant parameters of climatological importance.

References:

Adler, et al, (2003): The version 2 Global Precipitation Climatology Project (GPCP) monthly precipitation analysis (1979-Present). *J. Hydrometeor*, **4,** 1147-1167.

Anyamba, et al, (2001): NDVI anomaly patterns over Africa during the 1997/98 ENSO warm event. *Int. J. Remote Sensing*, **22,**1847–1859.

Bannu, et al (2007): Influence of El Niño and Indian Ocean dipole mode on the regional rainfall in Indonesia, *J.Clim.,* (submitted).

Hendon, H.H, (2003): Indonesian rainfall variability: impacts of ENSO and local air-sea interaction. *J. Climate*, **16**, 1775-1790.

Kalnay, E., and coauthors, 1996: The NCEP/NCAR 40-year reanalysis project. *Bull. Amer. Meteor. Soc.*, **77**, 437-471.

Miller et al., 1992: The sensitivity of the ECMWF model to the parameterization of evaporation from the tropical oceans. *J. Climate*, **5**, 418–434.

McBride, J. L, et al, (2003): Relationships between the Maritime Continent Heat Source and the El Niño-Southern Oscillation Phenomenon. *J. Clim,* **16**, 2905-2914.

MSC, (2002): Analysis and use of meteorological satellite images, Japan Meteorological Agency.

Qu, T. et al, (2005): Sea surface temperature and its variability in the Indonesian region, *Oceanography*, **18:4**, 50-61.

Rasmusson, E.M., and T.H. Carpenter, (1982): Variations in tropical sea surface temperature and surface wind fields associated with the Southern Oscillation/El Niño. *Mon. Wea. Rev.*, **110**, 354-384.

Ropelewski, C. F. and M. S. Halpert, (1987): Global and regional scale precipitation patterns associated with the El Niño/Southern Oscillation. *Mon. Wea. Rev.*, **115,** 1606–1626.

Smith, T. M., and R. W. Reynolds (2005), A global merged land air and sea surface temperature reconstruction based on historical observations (1880-1997). *J. Clim.*, **18**, 2021-2036.

Saji, et al, (1999): A dipole mode in the tropical Indian ocean, *Nature*, **401**, 360-363.